

## Ultramicroporous silicon nitride ceramics for CO<sub>2</sub> capture

Cristina Schitco<sup>a)</sup>

*Fachbereich Material-und Geowissenschaften, Technische Universität Darmstadt, 64287 Darmstadt, Germany*

Mahdi Seifollahi Bazarjani

*Fachgebiet Keramische Werkstoffe, Fakultät III Prozesswissenschaften, Institut für Werkstoffwissenschaften und -technologien, Technische Universität Berlin, 10623 Berlin, Germany*

Ralf Riedel

*Fachbereich Material-und Geowissenschaften, Technische Universität Darmstadt, 64287 Darmstadt, Germany*

Aleksander Gurlo

*Fachgebiet Keramische Werkstoffe, Fakultät III Prozesswissenschaften, Institut für Werkstoffwissenschaften und -technologien, Technische Universität Berlin, 10623 Berlin, Germany*

(Received 15 February 2015; accepted 19 May 2015)

Carbon dioxide (CO<sub>2</sub>) capture is regarded as one of the biggest challenges of the 21st century; therefore, intense research effort has been dedicated in the area of developing new materials for efficient CO<sub>2</sub> capture. Here, we report high CO<sub>2</sub> capture capacity in the low region of applied CO<sub>2</sub> pressures observed with ultramicroporous silicon nitride-based material. The latter is synthesized by a facile one-step NH<sub>3</sub>-assisted thermolysis of a polysilazane. Our newly developed material for CO<sub>2</sub> capture has the following outstanding properties: (i) one of the highest CO<sub>2</sub> capture capacities per surface area of micropores, with a CO<sub>2</sub> uptake of 2.35 mmol g<sup>-1</sup> at 273 K and 1 bar (ii) a low isosteric heat of adsorption (27.6 kJ mol<sup>-1</sup>), which is independent from the fractional surface coverage of CO<sub>2</sub>. Furthermore, we demonstrate that the pore size plays a crucial role in elevating the CO<sub>2</sub> adsorption capacity, surpassing the effect of Brunauer–Emmett–Teller specific surface area.

### I. INTRODUCTION

The problem of carbon dioxide (CO<sub>2</sub>) capture is considered as one of the grand challenges of the 21st century.<sup>1,2</sup> CO<sub>2</sub> Capture and Storage (CCS) scheme is regarded as one of the most practical option to reduce CO<sub>2</sub> emissions.<sup>3–6</sup>

The current technology for the removal of CO<sub>2</sub> from flue gas is based on the capture of CO<sub>2</sub> by aqueous amines.<sup>7–9</sup> This technology is an energy-intensive process and environmentally not feasible because of water and solvent recycling issues, as well as because of the corrosive interaction of oxygen and acidic components of the combustion gas with amines.<sup>3,10</sup> The alternative technology for the CO<sub>2</sub> capture is based on the storage of CO<sub>2</sub> in light-weight solid materials, involving two mechanisms: (i) chemisorption, hereby, CO<sub>2</sub> molecules interact chemically with functional groups (e.g., open-metal sites or amines) forming strong bonds, (ii) physisorption, CO<sub>2</sub> molecules adsorb in the pores.<sup>3,4</sup>

Materials with chemisorption mechanism adsorb CO<sub>2</sub> selectively even in the presence of other gases and can operate at high temperatures, indicating advantages over solid materials, which operate by physisorption

mechanism.<sup>11–13</sup> These materials include amine-modified solid sorbents,<sup>12,14,15</sup> inorganic-based materials such as hydrotalcites,<sup>16</sup> lithium zirconates,<sup>17</sup> and partially, porous materials with unsaturated metal centers (UMCs).<sup>13</sup> Because of the rigid network of UMCs, the accessibility of CO<sub>2</sub> to the adsorption sites is restricted and thus, CO<sub>2</sub> is not adsorbed through a pure chemisorption mechanism. However, the increased ionic character of metal-oxygen bonds contained in UMCs forms adsorption sites with higher heats of adsorption than those characteristics normally for physisorption, which in turn are responsible for the additional uptake of CO<sub>2</sub>. The values of heats of adsorption fall slightly, as the sites with the highest affinity to CO<sub>2</sub> are filled.

The advantages of materials, which interact chemically with CO<sub>2</sub>, are counteracted by high-energy costs associated with the activation, regeneration, and recycling of the sorbent. In addition, the selectivity of chemisorption tends to monotonically decrease with increased loading of sorbate.<sup>18</sup>

Furthermore, recent studies have shown that the pressure/vacuum swing adsorption (PSA/VSA) technology is competitive for CO<sub>2</sub> capture because the energy consumptions are lower than those of amine processes.<sup>19</sup> The majority of investigations on CO<sub>2</sub> recovery based on VSA technology use adsorbents, which operate by physisorption mechanism (i.e., zeolites).<sup>20</sup> In addition, coal-fired power plants, which are the

Contributing Editor: Tania Paskova

<sup>a)</sup>Address all correspondence to this author.

e-mail: schitco@materials.tu-darmstadt.de

DOI: 10.1557/jmr.2015.165

largest source of CO<sub>2</sub> emission, produce flue gas at 1 bar with a CO<sub>2</sub> concentration of less than 15%.<sup>6,21</sup> Consequently, there is a need to develop thermally stable solid material characterized by a high-adsorption value and moderate heat of adsorption. These features could allow efficient CO<sub>2</sub> capture by physisorption in the low pressure region up to 1 bar suitable for postcombustion capture.<sup>13</sup>

In this regard, zeolites, activated carbons (ACs), and metal-organic materials (MOMs) have been commonly used for CO<sub>2</sub> capture by physisorption. Excellent CO<sub>2</sub> capture capacities at low temperatures or/and high pressures have been obtained for instance, by Maxsorb, an AC material and Zeolite 13X adsorbing approximately 13 mmol g<sup>-1</sup> at 298 K and 10 bars<sup>22</sup> and 3.9 mmol g<sup>-1</sup> at 298 K and 1 bar, respectively.<sup>23</sup>

Materials with high CO<sub>2</sub> capture capacity can be produced by the introduction of nitrogen-containing basic groups that interact with a weak acidic gas such as CO<sub>2</sub>. In this regard, the reaction with nitrogen-containing reagents, such as ammonia (NH<sub>3</sub>) and amines, is a common technique to create solid sorbents with high CO<sub>2</sub> capture capacity. For example, the functionalization of AC by nitrogen-containing basic groups has been extensively reported in the literature.<sup>20,24–26</sup> The incorporation of nitrogen-containing basic groups could create additional sites for the adsorption of CO<sub>2</sub>.<sup>24</sup>

However, in some cases, the functionalization of AC by amino/nitro groups has resulted in the decrease of Brunauer–Emmett–Teller (BET) surface area and micropore volume, leading to the drop of CO<sub>2</sub> capture capacity of nitrogen-modified adsorbent compared to that of the pristine sample.<sup>20</sup>

Recently, Zhao et al. has reported a facile synthesis of porous carbon nitride spheres with hierarchical three-dimensional mesostructures and nitrogen-containing groups for CO<sub>2</sub> capture.<sup>25</sup> The hierarchical porous spheres with BET surface area of ~550 m<sup>2</sup> g<sup>-1</sup> possess at 1 bar CO<sub>2</sub> capture capacity of 2.90 and 0.97 mmol g<sup>-1</sup> at 298 and 348 K, respectively. In comparison, the pristine-AC has a CO<sub>2</sub> capture capacity of 2.50 and 0.30 mmol g<sup>-1</sup> at 298 and 348 K, respectively. The enhanced CO<sub>2</sub> capture capacity is because of the presence of nitrogen-containing basic groups, together with hierarchical mesostructures, which include relatively high BET surface, stable framework, and the presence of a large number of micropores as well as small mesopores. However, the mechanism of CO<sub>2</sub> adsorption is not further described.

In analogy to the carbon nitride materials, silicon nitride, silicon diimide, and intermediate silicon imidonitride compositions are of great interest for CO<sub>2</sub> capture, especially at high temperature where carbonaceous materials fail to operate. However, the creation of nitrogen-containing silicon-based materials with high porosity is challenging.

Recently, a mesoporous silicon diimide with high CO<sub>2</sub> capture capacity was synthesized by the reaction of SiCl<sub>4</sub> and NH<sub>3</sub>.<sup>11</sup> The production of latter material requires vacuum and ammonia (NH<sub>3</sub>) with careful temperature-programmed treatment, which are costly for the large-scale applications.

High surface area materials derived from polymer-derived ceramics, including silicon nitrides are obtained when low pyrolysis temperatures are used. This is, during the polymer-to-ceramic transformation, the decomposition of organic groups, and the release of gaseous species, e.g., H<sub>2</sub>, CH<sub>4</sub>, occurs mainly at temperatures around 500–700 °C.<sup>27–29</sup> Hence, the evolution of these gaseous species creates an intrinsic microporosity in as-formed products. Stopping the pyrolysis at this conversion stage leads to microporous materials in a hybrid state called ceramers, i.e., the as-formed ceramic product contains reactive sites from the unconverted polymer.<sup>30,31</sup> Due to their microporosity and reactive sites, these materials are suited for applications, such as gas adsorption,<sup>31</sup> catalysis,<sup>32</sup> or gas separation membranes.<sup>33</sup>

Here, we report the high CO<sub>2</sub> capture capacity of microporous silicon nitride materials, which are produced by a facile one-step NH<sub>3</sub>-assisted thermolysis from a preceramic polymer.

The ideal material for CO<sub>2</sub> capture based on physisorption mechanism should (i) be thermally stable, (ii) have high-adsorption capacity in the low-pressure region (up to 1 bar), and (iii) possess moderate heat of adsorption over a wide temperature range and loading of sorbate.

However, the development of a high-capacity CO<sub>2</sub> storage system with above-mentioned properties is hindered because of the poor understanding of the pore size and specific surface area (SSA) requirements in correlations with CO<sub>2</sub> uptake. Furthermore, it is assumed that the adsorption capacity of a material, which operates by physisorption, can be enhanced only by increasing the BET SSA. Here, we demonstrate that the pore size could play a crucial role in elevating the CO<sub>2</sub> adsorption capacity surpassing the effect of BET SSA.

In this article, we report high CO<sub>2</sub> storage capacity over a wide range of applied CO<sub>2</sub> pressures for a silicon nitride material, which is ultramicroporous. On the contrary to other CO<sub>2</sub> capture systems, this silicon nitride material has a low surface area (BET surface area of 230 m<sup>2</sup> g<sup>-1</sup> as measured by N<sub>2</sub> physisorption).

## II. EXPERIMENTAL SECTION

### A. Materials

For the synthesis of ultramicroporous silicon nitride material, the commercially available polysilazane HTT-1800 (KION Specialty Polymers) has been applied as starting material. The polymer is handled under an inert atmosphere using Schlenk techniques. Polymer

pyrolysis is carried out in a horizontal tube furnace, by placing the sample in a quartz crucible inside a quartz tube. The ultramicroporous silicon nitride material, labeled HTT600NH, is produced by thermolysis under an NH<sub>3</sub> atmosphere at 600 °C for 1 h with a heating rate of 100 °C h<sup>-1</sup>.

## B. Structural characterization and elemental analysis

X-ray diffraction (XRD) was carried out using a STOE x-ray diffractometer (Darmstadt, Germany) equipped with a MoK<sub>α</sub> radiation. Attenuated total reflection Fourier transform infrared spectroscopy (ATR-FTIR) spectrum was recorded on a Varian 670-IR (Agilent Technologies) using 0.5 of powdered sample. The sample preparation was performed in glovebox under an inert atmosphere to avoid the contact with moisture.

The carbon content was determined in a carbon analyzer CS-800 (ELTRA GmbH, Haan, Germany), the nitrogen and oxygen content in an N/O analyzer Leco TC-436 (Leco Corporation, St. Joseph, MI). The hydrogen content was determined by the Mikroanalytisches Labor Pascher (Remagen, Germany) using the coupled plasma atomic emission spectroscopy (Thermo Instruments, iCAP 6500, Waltham, MA) and element analyzer (Pascher). The silicon content was calculated from the sum of constituting elements.

## C. Gas adsorption

N<sub>2</sub> adsorption was performed at 77 K using an Autosorb-3B (Quantachrome Instruments, Boynton Beach, FL). The sample was preheated at 423 K for 24 h under vacuum before the measurements. The N<sub>2</sub> physisorption isotherm at 77 K was used to calculate the SSA from the linear BET plots over the range of 0.05 <  $p/p_0$  < 0.3. The total pore volume ( $V_T$ ) was determined from the amount of vapor adsorbed at the relative pressure of  $p/p_0 \sim 1$ . The micropore volume ( $V_{\text{micro}}$ ) was calculated using the deBoer's  $t$ -plot analysis.

CO<sub>2</sub> adsorption analysis was performed at 273 K by an ASAP-2000 automated volumetric analyzer (Micromeritics Instrument Corporation, Norcross, GA) using the same outgassing procedure mentioned for N<sub>2</sub> adsorption. Ultramicropore volume ( $V_{\text{ultra}}$ ) was calculated by applying the Dubinin–Astakhov (D–A) equation to the CO<sub>2</sub> adsorption isotherm at 273 K. Mean pore size ( $d$ ) was estimated by the equation of Stoekli for the characteristic adsorption potential between 20 and 42 kJ mol<sup>-1</sup>, the latter being determined as well by D–A equation from the CO<sub>2</sub> isotherm at 273 K. For more details, please refer to our previous work.<sup>34</sup>

High pressure CO<sub>2</sub> adsorption isotherms were recorded with an automated high-pressure volumetric sorption analyzer iSorb (Quantachrome Instruments, Boynton Beach, FL). Prior to the adsorption run, the void volume

of the sample cell was determined in a blank cell measurement under given analyses conditions. The sample was degassed at 100 °C for 12 h. The measured adsorption data were corrected by the blank cell measurement. The contact of the sample with ambient air was reduced to a minimum <10 min.

### 1. Calculation of isosteric heat of adsorption ( $Q_{\text{st}}$ )

High pressure CO<sub>2</sub> adsorption isotherms of HTT600NH were fitted by the Tóth equation [Eq. (1)] at 273 K [Fig. S1(a) in Supplementary Material] and 373 K [Fig. S1(b) in Supplementary Material] up to 15 bars. Only part of the isotherm showing the characteristics of type I isotherm, which corresponds to micropore filling was fitted by the Tóth equation. The part corresponding to micropore filling region was found for both isotherms (recorded at 273 and 373 K, respectively) to be up to 15 bars. Beyond this pressure, the isotherms showed a steep rise, evidence that the CO<sub>2</sub> molecules were filling the interparticle distances or the macropores of the silicon nitride material (Fig. S1 in Supplementary Material). Prior to the fitting procedure, the isotherm recorded at 373 K [Fig. 3(a)] was interpolated by using b-cubic spline method.

The Tóth equation<sup>35</sup> has been originally proposed for monolayer adsorption by Tóth, providing a more extensive range of fit compared to that of the Langmuir or Freundlich equation when applied to type I isotherms. The Tóth equation has the advantage to satisfy both limits of the isotherm, at  $p \rightarrow 0$  and  $p \rightarrow \infty$ . The expression is given by:

$$n = n_m \left( \frac{(kp)^m}{1 + (kp)^m} \right)^{1/m}, \quad (1)$$

where  $n$  and  $n_m$  are the number of mole adsorbed at a given pressure and the number of moles adsorbed at saturation, respectively.  $p$  is the pressure, and  $k$  and  $m$  are the constants.

The parameters are specific for adsorbent–adsorbate pairs, and  $m$  is less than 1 for heterogenous adsorbents. When  $m$  is equal to 1, the Tóth equation reduces to the Langmuir equation. The Tóth equation is used to fit the CO<sub>2</sub> adsorption isotherm of HTT600NH because of its simplicity and correct behavior at both low and high pressure ranges of the adsorption isotherm. Many isotherm data of ACs and zeolites are well fitted and represented by the Tóth equation.

The  $Q_{\text{st}}$  as a function of fractional surface coverage is determined by fitting the isotherm of HTT600NH at 273 and 373 K with the Tóth equation and by using the Clausius–Clayperon equation (CC).  $Q_{\text{st}}$  is a key parameter in determining the difference between chemical and physical adsorption. The magnitude of  $Q_{\text{st}}$  determines the strength of the bond formed between the adsorbate and

the adsorbent.  $Q_{st}$  could be a function of the amount of the adsorbed species, so-called fractional surface coverage ( $\theta$ ).

Different behaviors are observed for various systems.  $Q_{st}$  remains either constant with  $\theta$  or it decreases linearly or exponentially with  $\theta$ . The latter behavior is because of the heterogeneity of energy distributions, that is, the molecules tend to adsorb first on sites with the maximum free energy change (maximum heat of adsorption). So a gradual decrease of  $Q_{st}$  with  $\theta$  indicates that the higher energy sites are becoming occupied.

The heat of adsorption ( $\Delta H$ ) from the adsorption isotherms can be estimated with the help of CC equation. The CC equation is used extensively in vapor–liquid equilibrium and is based on the assumption of an ideal gas. Here, the specific volume of the liquid is very small compared to the volume of gas, and the equation can be written as:

$$\frac{d \ln p}{dT} = \frac{\Delta H}{RT^2} \quad (2)$$

where  $R$  is the gas constant, and  $T$  is the temperature.

In adsorption equilibrium, the equilibrium pressure is a function of the amount of adsorbed species. Consequently, the isosteric heat of adsorption ( $Q_{st}$ ) at a specified level of surface coverage is a function of the fractional surface coverage ( $\theta$ ). Thus,  $Q_{st}$  could be estimated by the integration of Eq. (2):

$$\ln \left( \frac{p_1}{p_2} \right)_{\theta_1} = \frac{Q_{st}}{R} \left( \frac{1}{T_2} - \frac{1}{T_1} \right) \quad (3)$$

The  $Q_{st}$  calculated from the Eq. (3) corresponds to the fractional surface coverage of  $\theta_1$ . The variation of  $Q_{st}$  with  $\theta$  is determined by applying Eq. (3) for different levels of fractional surface coverage.

### III. RESULTS AND DISCUSSION

#### A. Structure and composition

The XRD pattern [Fig. 1(a)] of HTT600NH specimen indicates the formation of an amorphous material.

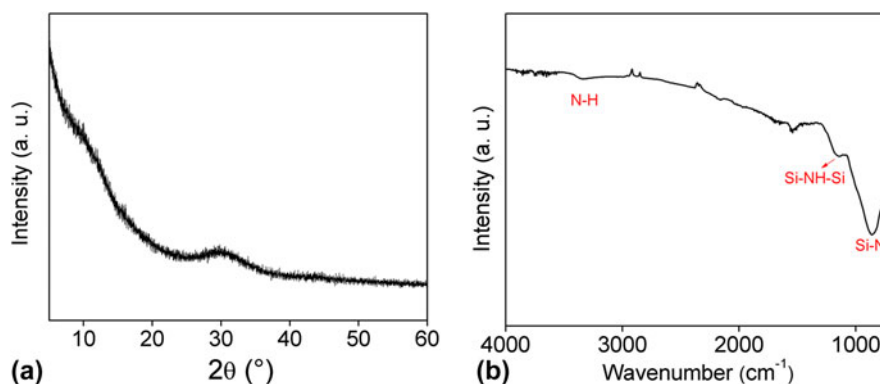


FIG. 1. (a) XRD pattern (the data were shown in Fig. 2 in Ref. 34) and (b) ATR-FTIR spectrum of HTT600NH specimen.

The results of the elemental analysis show the following atomic (weight) composition for HTT600NH: Si 36.9 (68.7), C 4.4 (3.6), N 23.2 (21.5), O 3.7 (4.1), and H 31.7 (2.1), corresponding to SiN<sub>0.63</sub>C<sub>0.12</sub>O<sub>0.10</sub>H<sub>0.86</sub> formula. The ATR-FTIR spectra [Fig. 1(b)] confirm the formation of a silicon imidonitride structure in the HTT600NH specimen:  $\nu = 3387$  [w;  $\nu$  (NH)], 1185 [m;  $\gamma$  (NH)], and 1000–900 (s; SiNSi).

#### B. Porosity characterization as revealed by gas adsorption

We have recently investigated the HTT600NH sample by gas adsorption techniques using N<sub>2</sub> and CO<sub>2</sub> as probe molecules, which reveal that the micropore volume contributes to 93% of the  $V_T$  of the sample, thus the HTT600NH sample is mainly microporous.<sup>34</sup>

HTT600NH specimen has a BET SSA of 230 m<sup>2</sup> g<sup>-1</sup>, far lower than that of 1009 m<sup>2</sup> g<sup>-1</sup>, found by Tsang et al. for a mesoporous silicon nitride,<sup>11</sup> and the extra-large SSA values up to 7000 m<sup>2</sup> g<sup>-1</sup>, reported for MOFs, zeolites or ACs.<sup>18</sup>

The  $V_T$ , determined from the N<sub>2</sub> adsorption isotherm [Fig. 2(a)] at the relative pressure of  $p/p_0 \approx 1.0$ , has a value of 0.14 cm<sup>3</sup> g<sup>-1</sup>. In comparison, the deBoer's  $t$ -plot analysis of the N<sub>2</sub> physisorption isotherm indicates the micropore volume ( $V_{micro}$ ) of 0.13 cm<sup>3</sup> g<sup>-1</sup>.<sup>34</sup> The D–A analysis of CO<sub>2</sub> adsorption isotherm for HTT600NH at subatmospheric pressures shows  $V_{ultra}$  and micropore size ( $d$ ) of 0.26 cm<sup>3</sup> g<sup>-1</sup> and 0.5 nm, respectively.<sup>34</sup> The porosity characteristics of HTT600NH are mentioned in Table I. In addition, micropores can be divided to ultramicropores (pores below 0.7 nm) and supermicropores (pores between 0.7 and 2 nm).<sup>36</sup> The recent analyses of aforementioned gas adsorption studies of the HTT600NH sample reveal that the ultramicropores are accounted approximately for a micropore volume of 0.26 cm<sup>3</sup> g<sup>-1</sup>, which is twice the micropore volume associated with supermicropores (0.13 cm<sup>3</sup> g<sup>-1</sup>). This indicates that ultramicroporosity contributes to about



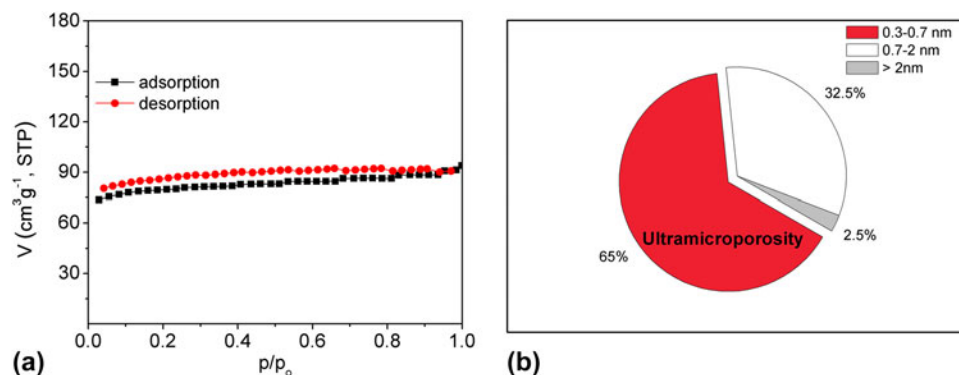


FIG. 2. (a) N<sub>2</sub> physisorption isotherm (the data were shown in Fig. 3(b) in Ref. 34) and (b) the pore fractions as determined by CO<sub>2</sub> and N<sub>2</sub> physisorption methods of HTT600NH specimen (the data were shown in Table 3 and Fig. 5 in Ref. 34).

TABLE I. The porosity characteristics of HTT600NH specimen.

Sample	SSA (m <sup>2</sup> g <sup>-1</sup> )	V <sub>T</sub> (cm <sup>3</sup> g <sup>-1</sup> )	V <sub>micro</sub> (cm <sup>3</sup> g <sup>-1</sup> )	V <sub>ultra</sub> (cm <sup>3</sup> g <sup>-1</sup> )	d (nm)
HTT600NH	230	0.14	0.13	0.26	0.5

65% of the total micropore volume in the HTT600NH specimen [Fig. 2(b)].<sup>34</sup>

### C. High pressure CO<sub>2</sub> adsorption

The CO<sub>2</sub> adsorption capacity of HTT600NH is measured at 273 and 373 K up to ~30 and 100 bars, respectively. The adsorption isotherm of HTT600NH at 273 K is similar to a typical type I profile up to 15 bars [Fig. 3(a)] found in microporous solids. The CO<sub>2</sub> adsorption isotherm of HTT600NH at 273 K has a saturation value of 3.26 mmol g<sup>-1</sup> at around 10 bars inferring that micropores are filled completely with CO<sub>2</sub>. The isotherm of HTT600NH at 273 K rises rapidly at pressures higher than 15 bars, which indicates that CO<sub>2</sub> fills the interparticle macropores, and micropores are already completely filled.

As HTT600NH specimen is mainly microporous, it is expected that the CO<sub>2</sub> uptake becomes saturated at relatively low pressures as a result of the saturation of micropores. Indeed, HTT600NH shows a CO<sub>2</sub> uptake of 2.35 mmol g<sup>-1</sup> at 273 K and 1 bar, a value which is twice as high as the minimum value needed for an effective CO<sub>2</sub> capture material.<sup>14</sup> The CO<sub>2</sub> uptake of HTT600NH (2.35 mmol g<sup>-1</sup> at 273 K and 1 bar) is comparable to that of typical CO<sub>2</sub> solid adsorbents with much larger SSA measured at 1 bar but at a slightly higher temperature of 298 K. For example, at 1 bar and 298 K, the CO<sub>2</sub> uptakes for Zeolite 13X, MSIN-673, and AC are 3.9, 2.6, and 2.1 mmol g<sup>-1</sup>, respectively.<sup>11</sup> The highest gravimetric CO<sub>2</sub> uptake of 5.41 mmol g<sup>-1</sup> at 1 bar and 298 K is reported for SIFSIX-2-Cu-i.<sup>18</sup> An interesting ultramicroporous MOM SIFSIX-3Zn with porosity characteristics similar to that of HTT600NH

has been reported by Uemura et al. in 2009.<sup>37</sup> Although the latter material exhibits a pore size and a BET surface area of only 3.84 Å and 250 m<sup>2</sup> g<sup>-1</sup>, respectively, as determined by CO<sub>2</sub> adsorption method, it possesses a high CO<sub>2</sub> uptake at 298 K and 1 bar of 2.54 mmol g<sup>-1</sup>.<sup>18</sup>

At 373 K, the CO<sub>2</sub> adsorption isotherm recorded up to 100 bars [Fig. 3(a)] indicates a drastic reduction of the CO<sub>2</sub> uptake, which is less than 0.5 and 1.2 mmol g<sup>-1</sup> at 1 bar and 10 bars, respectively, that is, a typical characteristic of physisorption. The dominance of physisorption mechanism is confirmed further by the isosteric heat of adsorption ( $Q_{st}$ ) of this material [Fig. 3(b)]. Figure 3(b) represents the  $Q_{st}$  as a function of different levels of fractional surface coverage ( $\theta$ ) for the CO<sub>2</sub> adsorption of HTT600NH calculated from adsorption isotherms at 273 and 373 K.

The low value of  $Q_{st}$ , which is 27.6 kJ mol<sup>-1</sup>, confirms the dominant role of physisorption during the CO<sub>2</sub> uptake in HTT600NH. The relatively constant  $Q_{st}$  over the complete range of CO<sub>2</sub> uptake infers homogeneous adsorption sites (see Experimental section). These  $Q_{st}$  values are in the favorable range for an efficient reversible adsorption-desorption process.<sup>18</sup> By contrast, the mesoporous silicon nitride MSIN-673, which is reported by Tsang et al.,<sup>11</sup> exhibits chemisorption characteristics inferred from the exponential reduction of  $Q_{st}$  with fractional surface coverage ( $\theta$ ). In addition, for MSIN-673, the highest  $Q_{st}$  value that is estimated at the lowest CO<sub>2</sub> surface coverage is 68.1 kJ mol<sup>-1</sup>, while at higher surface coverages, the  $Q_{st}$  converges to a value of 40–50 kJ mol<sup>-1</sup>.

The high reversibility of CO<sub>2</sub> adsorption for HTT600NH at 273 and 373 K and pressure ranges are demonstrated in Fig. 4. However, the desorption isotherm does not exactly follow the adsorption isotherm, which could be caused by imide sites with high affinity toward CO<sub>2</sub> (chemisorption) or the entrapment of CO<sub>2</sub> in the pores. Whatsoever, the amount of CO<sub>2</sub> trapped in

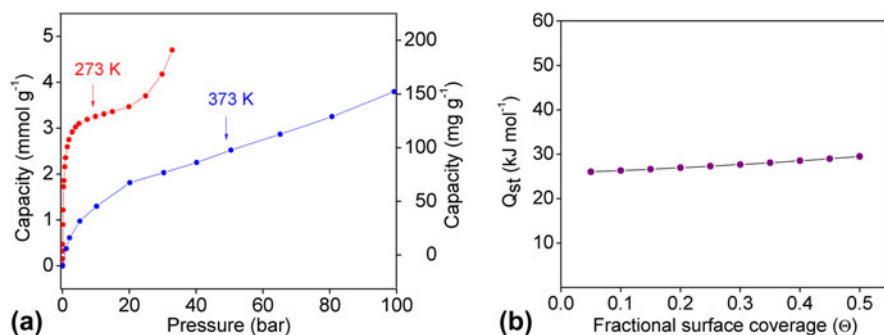


FIG. 3. (a) CO<sub>2</sub> adsorption isotherm of HTT600NH at 273 K (red) and at 373 K (blue), the primary and secondary Y-axes indicate CO<sub>2</sub> adsorption capacity of HTT600NH with units of mmol g<sup>-1</sup> and mg g<sup>-1</sup>, respectively and (b) isosteric heats of adsorption ( $Q_{st}$ ) of HTT600NH as a function of fractional surface coverage ( $\theta$ ).

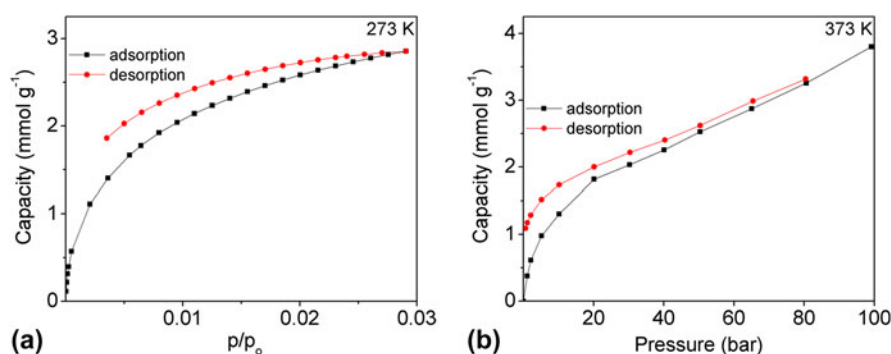


FIG. 4. (a) CO<sub>2</sub> isotherms of HTT600NH at 273 K and up to 1 bar (the data were shown in Fig. 3(d) in Ref. 34) and (b) CO<sub>2</sub> adsorption-desorption isotherms of HTT600NH at 373 K and up to 100 bar.

the material after desorption decreases with increasing temperature, a strong evidence that physisorption mechanism is dominant.

The open-metal sites or amine functional groups interact chemically with CO<sub>2</sub>, promoting chemisorption, which is associated with high heats of adsorption (>45 kJ mol<sup>-1</sup>), leading to high energy costs for the regeneration of the material.<sup>38</sup> In our study, although the HTT600NH contains residual imide groups, it possesses a low  $Q_{st}$ . This provides further evidence that in the HTT600NH, micropores play a major role for CO<sub>2</sub> adsorption by physisorption mechanism as a result of the presence of homogenous adsorption sites, i.e., ultramicropores. Although the adsorption occurs by physisorption, the appearance of hysteresis loop is because of the similar kinetic diameter of CO<sub>2</sub> and the pore dimension, reducing the complete desorption of CO<sub>2</sub> during the measurement time. However, such a hysteresis may be not always a problem and can point out to an interesting storage material.<sup>4</sup>

#### D. Correlation of CO<sub>2</sub> storage capacity with the pore size

The aforementioned role of micropores on the adsorption of CO<sub>2</sub> can be better realized by the

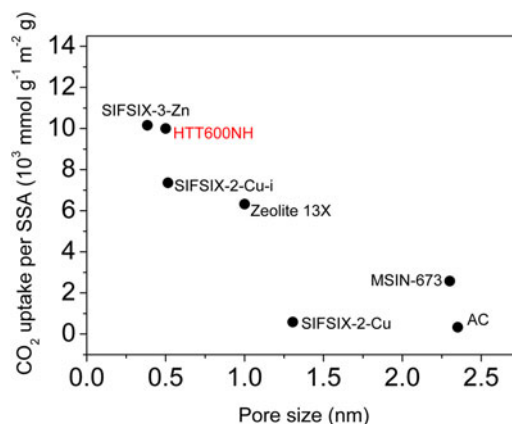


FIG. 5. CO<sub>2</sub> uptake normalized by SSA versus average pore size for HTT600NH (273 K, 1 bar) and representative examples from literature, MOMs<sup>18</sup>: SIFSIX-3Zn, SIFSIX-2-Cu-i, SIFSIX-2-Cu (293 K, 1 bar); Zeolites<sup>3,12</sup>: Zeolite 13X (293 K, 1 bar); Nitrides<sup>11</sup>: MSIN-673 (293 K, 1 bar); ACs<sup>44</sup>: AC (293 K, 1 bar), for details see Table S1.

correlation of storage capacity with pore size. This is demonstrated by normalizing the CO<sub>2</sub> uptake of a material with its SSA and plotting it as a function of pore size. This correlation is found by using the CO<sub>2</sub> uptake for HTT600NH at 273 K and 1 bar, as

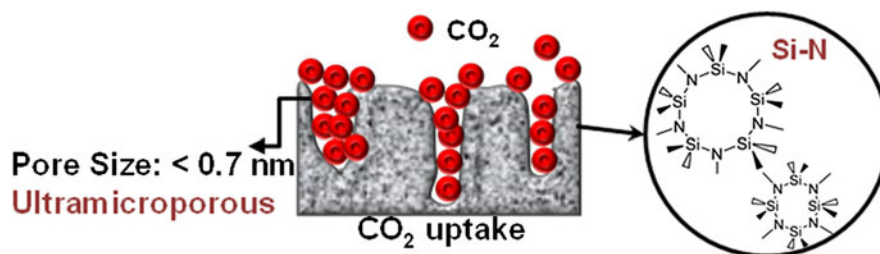


FIG. 6. Schematic representation of CO<sub>2</sub> capture on ultramicroporous silicon nitride.

well as for representative selected materials, e.g., MOFs, Zeolite, AC, and nitrides from literature (Fig. 5 and Table SI from Supplementary Material). Figure 5 reveals unambiguously that HTT600NH has nearly the highest CO<sub>2</sub> uptake per BET SSA. Therefore, the ultramicropores provide the greatest contribution to total capacity for CO<sub>2</sub> uptake, which is not directly connected to the BET SSA of material as represented in Fig. 6. This is explained as follows. It is known that BET SSA as determined by N<sub>2</sub> physisorption at 77 K does not necessarily account for narrow microporosity, i.e., ultramicroporosity. This may be caused by three factors:

(i) N<sub>2</sub> molecules are adsorbed in macropores, mesopores, and micropores by three different mechanisms—multilayer adsorption, capillary condensation, and micropore filling, respectively.<sup>36</sup> The calculation of SSA by the BET method assumes that N<sub>2</sub> molecules are adsorbed by the capillary condensation mechanism. Hence, the validity of BET SSA is restricted mostly to mesoporous materials. It is generally agreed that BET SSA does not reflect the true values of microporous materials or micro-/mesoporous materials, but it is widely accepted to be used for comparison purposes.<sup>39,40</sup>

(ii) The maximum size of ultramicropores corresponds to the bilayer thickness of nitrogen molecules<sup>36</sup>; therefore, the adsorbed N<sub>2</sub> molecules near the entrance to the pore may block further adsorption, as it has been already evidenced in the work of Uemura et al.,<sup>37</sup> leading to the underestimation of the real value of SSA of the microporous material. It is generally agreed that N<sub>2</sub> molecule does not reflect well the ultramicroporosity, and for this purpose, other probe molecules such as H<sub>2</sub>, Ar, or CO<sub>2</sub> are preferred.<sup>41–43</sup>

(iii) Variation in the polarity and/or nature of pore surfaces may lead to wrong SSA values (either overestimated or underestimated). For instance, the interaction of N<sub>2</sub> with polar surfaces leads to smaller cross-sectional area of N<sub>2</sub>, if compared to the standard value of 0.135 versus 0.165 nm<sup>2</sup>, respectively.<sup>42</sup>

#### IV. CONCLUSION

A silicon nitride material has been successfully synthesized by a facile NH<sub>3</sub>-assisted thermolysis technique. We have shown that ultramicroporous HTT600NH has a high capacity for CO<sub>2</sub> adsorption. At 273 K and 1 bar, the CO<sub>2</sub> uptake corresponds to a value of 2.35 mmol g<sup>-1</sup> and is associated with the low isosteric heat of adsorption of 27.6 kJ mol<sup>-1</sup>. In addition, we believe that the CO<sub>2</sub> uptake is strongly correlated with the pore size rather than the BET SSA of a material. We propose that high CO<sub>2</sub> storage capacities by physisorption at 273 K and up to 1 bar can be achieved in materials with high amount of ultramicropore volume. Therefore, to achieve an enhanced CO<sub>2</sub> uptake at low temperatures, e.g., 273–298 K, and pressures up to 1 bar, the material development should follow the direction of maximizing the SSA and pore volume of the pores in ultramicroporous range. On the other hand, high CO<sub>2</sub> uptake capacities at high pressures could be achieved in large SSA materials due to the contribution of supermicropores and mesopores.

#### ACKNOWLEDGMENTS

The research leading to these results has received funding from the European Union Seventh Framework Program (FP7/2007-2013) under grant agreement no 264873 (FUNEA – Functional Nitrides for Energy Applications). The authors would like to acknowledge Duan Li and Professor James Shen for their assistance in CO<sub>2</sub> adsorption measurements.

#### REFERENCES

1. M.Z. Jacobson: Review of solutions to global warming, air pollution, and energy security. *Energy Environ. Sci.* **2**(2), 148 (2009).
2. D.M. D'Alessandro, B. Smit, and J.R. Long: Carbon dioxide capture: Prospects for new materials. *Angew. Chem., Int. Ed.* **49**(35), 6058 (2010).
3. Z. Liang, M. Marshall, and A.L. Chaffee: CO<sub>2</sub> adsorption-based separation by metal organic framework (Cu-BTC) versus zeolite (13X). *Energy Fuels* **23**(5), 2785 (2009).

4. R.E. Morris and P.S. Wheatley: Gas storage in nanoporous materials. *Angew. Chem., Int. Ed.* **47**(27), 4966 (2008).
5. I.E. Agency: *Prospects for Carbon Dioxide Capture and Storage* (International Energy Agency, Organisation for Economic Cooperation and Development, Paris, 2004).
6. E.J. Granite and H.W. Pennline: Photochemical removal of mercury from flue gas. *Ind. Eng. Chem. Res.* **41**(22), 5470 (2002).
7. P. Markewitz, W. Kuckshinrichs, W. Leitner, J. Linssen, P. Zapp, R. Bongartz, A. Schreiber, and T.E. Muller: Worldwide innovations in the development of carbon capture technologies and the utilization of CO<sub>2</sub>. *Energy Environ. Sci.* **5**(6), 7281 (2012).
8. A.L. Kohl and R. Nielsen: *Gas Purification* (Gulf Pub., Houston, 1997).
9. A.J. Hunt, E.H.K. Sin, R. Marriott, and J.H. Clark: Generation, capture, and utilization of industrial carbon dioxide. *ChemSusChem* **3**(3), 306 (2010).
10. A. Sayari and Y. Belmabkhout: Stabilization of amine-containing CO<sub>2</sub> adsorbents: Dramatic effect of water vapor. *J. Am. Chem. Soc.* **132**(18), 6312 (2010).
11. H.W. Yang, A.M. Khan, Y.Z. Yuan, and S.C. Tsang: Mesoporous silicon nitride for reversible CO<sub>2</sub> capture. *Chem. Asian J.* **7**(3), 498 (2012).
12. P.D. Jadhav, R.V. Chatti, R.B. Biniwale, N.K. Labhsetwar, S. Devotta, and S.S. Rayalu: Monoethanol amine modified zeolite 13X for CO<sub>2</sub> adsorption at different temperatures. *Energy Fuels* **21**(6), 3555 (2007).
13. S.R. Caskey, A.G. Wong-Foy, and A.J. Matzger: Dramatic tuning of carbon dioxide uptake via metal substitution in a coordination polymer with cylindrical pores. *J. Am. Chem. Soc.* **130**(33), 10870 (2008).
14. R.A. Khatri, S.S.C. Chuang, Y. Soong, and M. Gray: Thermal and chemical stability of regenerable solid amine sorbent for CO<sub>2</sub> capture. *Energy Fuels* **20**(4), 1514 (2006).
15. S. Satyapal, T. Filburn, J. Trela, and J. Strange: Performance and properties of a solid amine sorbent for carbon dioxide removal in space life support applications. *Energy Fuels* **15**(2), 250 (2001).
16. N.D. Hutson, S.A. Speakman, and E.A. Payzant: Structural effects on the high temperature adsorption of CO<sub>2</sub> on a synthetic hydro-talcite. *Chem. Mater.* **16**(21), 4135 (2004).
17. E. Ochoa-Fernández, M. Rønning, T. Grande, and D. Chen: Synthesis and CO<sub>2</sub> capture properties of nanocrystalline lithium zirconate. *Chem. Mater.* **18**(25), 6037 (2006).
18. P. Nugent, Y. Belmabkhout, S.D. Burd, A.J. Cairns, R. Luebke, K. Forrest, T. Pham, S. Ma, B. Space, L. Wojtas, M. Eddaoudi, and M.J. Zaworotko: Porous materials with optimal adsorption thermodynamics and kinetics for CO<sub>2</sub> separation. *Nature* **495**(7439), 80 (2013).
19. J. Merel, M. Clausse, and F. Meunier: Experimental investigation on CO<sub>2</sub> post-combustion capture by indirect thermal swing adsorption using 13X and 5A zeolites. *Ind. Eng. Chem. Res.* **47**(1), 209 (2008).
20. M.G. Plaza, C. Pevida, A. Arenillas, F. Rubiera, and J.J. Pis: CO<sub>2</sub> capture by adsorption with nitrogen enriched carbons. *Fuel* **86**(14), 2204 (2007).
21. E. Kintisch: Power generation - Making dirty coal plants cleaner. *Science* **317**(5835), 184 (2007).
22. S. Himeno, T. Komatsu, and S. Fujita: High-pressure adsorption equilibria of methane and carbon dioxide on several activated carbons. *J. Chem. Eng. Data* **50**(2), 369 (2005).
23. S.H. Hyun and R.P. Danner: Equilibrium adsorption of ethane, ethylene, isobutane, carbon-dioxide, and their binary-mixtures on 13X molecular-sieves. *J. Chem. Eng. Data* **27**(2), 196 (1982).
24. J.A. Thote, K.S. Iyer, R. Chatti, N.K. Labhsetwar, R.B. Biniwale, and S.S. Rayalu: In situ nitrogen enriched carbon for carbon dioxide capture. *Carbon* **48**(2), 396 (2010).
25. Q. Li, J. Yang, D. Feng, Z. Wu, Q. Wu, S.S. Park, C-S. Ha, and D. Zhao: Facile synthesis of porous carbon nitride spheres with hierarchical three-dimensional mesostructures for CO<sub>2</sub> capture. *Nano Res.* **3**(9), 632 (2010).
26. A.S. Jalilov, G. Ruan, C.C. Hwang, D.E. Schipper, J.J. Tour, Y. Li, H. Fei, E.L. Samuel, and J.M. Tour: Asphalt-derived high surface area activated porous carbons for carbon dioxide capture. *ACS Appl. Mater. Interfaces* **7**(2), 1376 (2015).
27. M. Seifollahi Bazarjani, H-J. Kleebe, M.M. Müller, C. Fasel, M. Baghaie Yazdi, A. Gurlo, and R. Riedel: Nanoporous silicon oxycarbonitride ceramics derived from polysilazanes in situ modified with nickel nanoparticles. *Chem. Mater.* **23**(18), 4112 (2011).
28. M.S. Bazarjani, M.M. Muller, H-J. Kleebe, C. Fasel, R. Riedel, and A. Gurlo: In situ formation of tungsten oxycarbide, tungsten carbide and tungsten nitride nanoparticles in micro- and mesoporous polymer-derived ceramics. *J. Mater. Chem. A* **2**(27), 10454 (2014).
29. P. Colombo: Engineering porosity in polymer-derived ceramics. *J. Eur. Ceram. Soc.* **28**(7), 1389 (2008).
30. H. Schmidt, D. Koch, G. Grathwohl, and P. Colombo: Micro-/macroporous ceramics from preceramic precursors. *J. Am. Ceram. Soc.* **84**(10), 2252 (2001).
31. M. Wilhelm, C. Soltmann, D. Koch, and G. Grathwohl: Ceramers - Functional materials for adsorption techniques. *J. Eur. Ceram. Soc.* **25**(2-3), 271 (2005).
32. J.S. Bradley, O. Vollmer, R. Rovai, U. Specht, and F. Lefebvre: High surface area silicon imidonitrides: A new class of microporous solid base. *Adv. Mater.* **10**(12), 938 (1998).
33. K. Miyajima, T. Eda, H. Ohta, Y. Ando, S. Nagaya, T. Ohba, and Y. Iwamoto: Development of Si-N based hydrogen separation membrane. In *Advances in Polymer Derived Ceramics and Composites*. (John Wiley & Sons, Hoboken, NJ, 2010); p. 87.
34. C. Schitco, M.S. Bazarjani, R. Riedel, and A. Gurlo: NH<sub>3</sub>-assisted synthesis of microporous silicon oxycarbonitride ceramics from preceramic polymers: A combined N<sub>2</sub> and CO<sub>2</sub> adsorption and small angle X-ray scattering study. *J. Mater. Chem. A* **3**(2), 805 (2015).
35. J. Toth: *Adsorption Theory, Modeling and Analysis* (Marcel Dekker, New York, 2002).
36. K. Kaneko: Determination of pore-size and pore-size distribution: I. Adsorbents and catalysts. *J. Membr. Sci.* **96**(1-2), 59 (1994).
37. K. Uemura, A. Maeda, T.K. Maji, P. Kanoo, and H. Kita: Syntheses, crystal structures and adsorption properties of ultramicroporous coordination polymers constructed from hexafluorosilicate ions and pyrazine. *Eur. J. Inorg. Chem.* **2009**(16), 2329 (2009).
38. K.A. Forrest, T. Pham, A. Hogan, K. McLaughlin, B. Tudor, P. Nugent, S.D. Burd, A. Mullen, C.R. Cioce, L. Wojtas, M.J. Zaworotko, and B. Space: Computational studies of CO<sub>2</sub> sorption and separation in an ultramicroporous metal-organic material. *J. Phys. Chem. C* **117**(34), 17687 (2013).
39. K.S.W. Sing, D.H. Everett, R.A.W. Haul, L. Moscou, R.A. Pierotti, J. Rouquerol, and T. Siemieniewska: Reporting physisorption data for gas solid systems with special reference



- to the determination of surface-area and porosity (Recommendations 1984). *Pure Appl. Chem.* **57**(4), 603 (1985).
40. H.M. Williams, E.A. Dawson, P.A. Barnes, B. Rand, R.M.D. Brydson, and A.R. Brough: High temperature ceramics for use in membrane reactors: The development of microporosity during the pyrolysis of polycarbosilanes. *J. Mater. Chem.* **12**(12), 3754 (2002).
41. D. Cazorla-Amorós, J. Alcañiz-Monge, and A. Linares-Solano: Characterization of activated carbon fibers by CO<sub>2</sub> adsorption. *Langmuir* **12**(11), 2820 (1996).
42. M. Thommes: Physical adsorption characterization of nanoporous materials. *Chem. Ing. Tech.* **82**(7), 1059 (2010).
43. J. Jagiello and M. Thommes: Comparison of DFT characterization methods based on N<sub>2</sub>, Ar, CO<sub>2</sub>, and H<sub>2</sub> adsorption applied to carbons with various pore size distributions. *Carbon* **42**(7), 1227 (2004).
44. C. Zhang, W. Song, G. Sun, L. Xie, J. Wang, K. Li, C. Sun, H. Liu, C.E. Snape, and T. Drage: CO<sub>2</sub> capture with activated carbon grafted by nitrogenous functional groups. *Energy Fuels* **27**(8), 4818 (2013).

### Supplementary Material

To view supplementary material for this article, please visit <http://dx.doi.org/jmr.2015.165>.